Near-Infrared Luminescence Spectroscopy of Nickelocene Doped into Single Crystals of Ruthenocene

Martin J. Davis and Christian Reber*

Département de chimie, Université de Montréal, Montréal, Québec, Canada H3C 3J7

Received November 22, 1994[⊗]

Single crystals of ruthenocene doped with nickelocene show a near-infrared luminescence band with a maximum at 13 100 cm^{-1} and a width of 1100 cm^{-1} at 5 K in addition to the ruthenocene luminescence. The band is symmetric and attributed to nickelocene on the basis of a comparison of luminescence and absorption spectra. Energy transfer from the ruthenocene host enhances the nickelocene luminescence intensity at temperatures between 50 and 100 K. An activation barrier of 306(18) cm^{-1} is determined from luminescence decay measurements. The Stokes shift of 2200 cm^{-1} and the large change of 0.16 Å in nickel−cyclopentadienyl distance in the emitting state confirm the assignment as $^3E_{1g}$, arising from an electron configuration different from that of the ground state. The comparison of experimental and calculated spectra shows that only low-energy vibrational modes contribute to the luminescence band shape, in contrast to the case of cobaltocene doped in the same host lattice, where a distortion along a high-frequency, ligand-centered mode affects the luminescence band shape.

Introduction

Metallocenes have been studied in great detail with respect to their chemical properties, including the synthesis and characterization of a wide variety of derivatives. There has been much interest in first-row metallocenes which form new classes of polymers and are applied in catalysis.[1,2] The properties of these materials often depend on details of their structure and dynamics.[1,2] Luminescence spectroscopy is a powerful method leading to new insight into ground and excited state properties of organometallics.[3] The technique has been mainly applied to second- and third-row metallocenes[3−6] and only to a much lesser extent to first-row metallocenes which often have their lowest-energy excited states in the near-infrared region, not accessible to routine luminescence spectrometers. In this study, we present and analyze the emission properties of nickelocene molecules doped into single crystals of ruthenocene.

We have previously given a detailed account of the luminescence properties of cobaltocene doped into single crystals of ruthenocene,[7] and the same spectroscopic approach is used for nickelocene in this report. The ruthenocene host lattice sensitizes the weak luminescence from the dopant metallocene and helps to separate dopant molecules from impurities which quench the luminescence in pure nickelocene. The intrinsic luminescence from ruthenocene is used to investigate energy transfer processes, another area that is very rarely explored for organometallic systems.

The nickel(II) ion in nickelocene has the [Ar]$3d^8$ electron configuration. The exact symmetry of the molecule in the ruthenocene host lattice is not known, but for consistency with literature, we use D_{5d} labels for orbitals and electronic states in the following.[8] In the electronic ground state, two of the 3d electrons are in the antibonding e_{1g} orbitals. The $^3A_{2g}$ ground state is orbitally nondegenerate and therefore not susceptible to a Jahn−Teller effect, in contrast to the case of cobaltocene, where we analyzed this effect in the luminescence spectrum.[7] The lowest energy excited states of nickelocene are $^3E_{1g}$ and $^1A_{1g}$, determined from solution absorption spectra and ligand-field calculations in the literature.[8,9] We present an assignment and analysis of the emitting state in the doped crystal based on our spectroscopic results. The comparison with the luminescence spectra of cobaltocene in the same host lattice shows the important spectroscopic differences between these two systems and illustrates the detailed excited state information that can be obtained even from unresolved spectra.

Experimental Section

Nickelocene and ruthenocene were obtained from Strem Chemicals and were purified by sublimation in sealed tubes. Nickelocene is sensitive to oxidation, and therefore all manipulations were carried out under a dry argon atmosphere in a glovebox. Doped crystals were prepared by cosublimation of ruthenocene and nickelocene in evacuated, sealed tubes. In a typical preparation, 200 mg of ruthenocene and 2 mg of nickelocene were mixed. The tubes were slowly lowered into a water bath held at 80 °C, and within 1 week pale green crystals with an edge length of about 2 mm were obtained. The doped crystals were formed by repeated sublimation and crystallization in progressively higher parts of the tube, thus contributing to the purification of the final crystals. The crystals show a varying intensity of their green color under a microscope, indicating an inhomogeneous distribution of the nickelocene molecules in the ruthenocene host lattice. The nickel content of some crystals was determined by atomic absorption spectrometry.

Luminescence and absorption spectra were recorded using instruments described in detail previously.[7] The samples used for spectroscopic experiments were placed in a helium gas, continuous-flow cryostat (Oxford Instruments CF 1204) with quartz windows. The temperature of the sample was determined with a Rh−Fe resistor on the sample holder. The excitation source was a 150 W Xe arc lamp (ICL LX-150UV) filtered through a 10 cm cell with quartz windows containing a 1 M copper sulfate solution to remove the IR radiation

[⊗] Abstract published in *Advance ACS Abstracts,* April 15, 1996.

(1) Foucher, D. A.; Tang, B. Z.; Manners, I. *J. Am. Chem. Soc.* **1992**, *114*, 6246.
(2) Nelson, J. M.; Rengel, H.; Manners, I. *J. Am. Chem. Soc*. **1993**, *115*, 7035.
(3) Lees, A. J. *Chem. Rev.* **1987**, *87*, 711.
(4) Perutz, R. *Chem. Soc. Rev.* **1993**, 361.
(5) Crosby, G. A.; Hager, G. D.; Hipps, K. W.; Stone, M. L. *Chem. Phys. Lett.* **1974**, *28*, 497.
(6) Hollingsworth, G. J.; Shin, K.-S. K.; Zink, J. I. *Inorg. Chem.* **1990**, *29*, 2501.
(7) Davis, M. J.; Reber, C. *Inorg. Chem.* **1995**, *34*, 4585.
(8) Gordon, K. R.; Warren, K. D. *Inorg. Chem.* **1978**, *17*, 987.
(9) Pavlik. L.; Cerny, V.; Maxova, E. *Collect. Czech. Chem. Commun.* **1970**, *35*, 3045.

S0020-1669(94)01346-7 CCC: $12.00

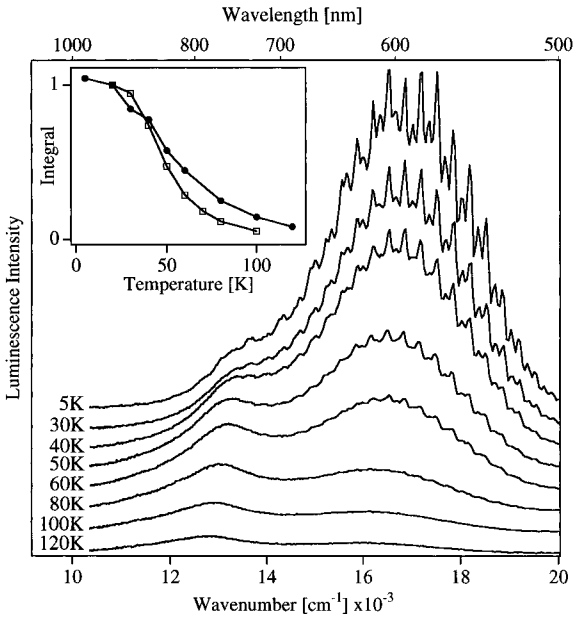

Figure 1. Single-crystal luminescence spectra of nickelocene doped into ruthenocene under broad-band ultraviolet excitation. Spectra recorded at temperatures between 5 and 120 K are shown. The inset shows integrated luminescence intensities for the doped crystals (solid circles) and for pure ruthenocene (open squares).

and a Schott UG11 filter, leading to an excitation wavelength range from 290 to 380 nm. The excitation light was focused onto the sample using quartz lenses. A Lumonics HyperEx-400 XeCl excimer laser with pulses of less than 20 ns duration at 308 nm, repetition rates between 15 and 30 Hz, and pulse energies of 1−5 mJ measured in front of the cryostat window was used for the luminescence decay measurements. The output from the photomultiplier (Hamamatsu R928) was terminated to 50−300 Ω and connected to a digital oscilloscope (HP54503A, 500 MHz), set to average 2048 pulses. A CW Ti−sapphire laser (Coherent 890) at a wavelength of 688.0 nm with a power of 5 mW was used in the selective excitation experiments. The luminescence signal was dispersed by a 1 m double monochromator (Instruments SA U 1000) and detected with a standard photomultiplier and photon-counting system. All luminescence spectra are corrected for system response as described in ref 7.

Spectroscopic Results

The luminescence spectra of nickelocene doped in ruthenocene at different temperatures are shown in Figure 1. The molar ratio of Ni/Ru in this crystal was 0.008. At the lowest temperatures, we observe a structured spectrum similar to the emission spectrum of pure ruthenocene reported in the literature.[5,6] The fine structure on the high-energy side of the structured luminescence band is identical to that of pure ruthenocene to within 10 cm^{-1}. The position of the band maximum and the overall width at half-height are identical to those for pure ruthenocene. A distinguishable second peak is observed on the low-energy side of the ruthenocene band at 13 100 cm^{-1} even at the lowest temperatures, indicating the presence of luminophores other than the host ruthenocene molecules. The two luminescence bands were reproduced with a lower concentration sample (Ni/Ru ratio 0.003, obtained from different batches of starting materials), leading to spectra very similar to those in Figure 1, evidence for dominant luminescence intensity from low-concentration domains of the inhomogeneously doped crystals. No near-infrared luminescence band was observed from a doped crystal with a high concentration of nickelocene (Ni/Ru ratio 0.211). We also note that samples of pure nickelocene showed no luminescence at temperatures above 5 K, most likely due to efficient energy transfer between metallocene centers and deactivation at deep traps.

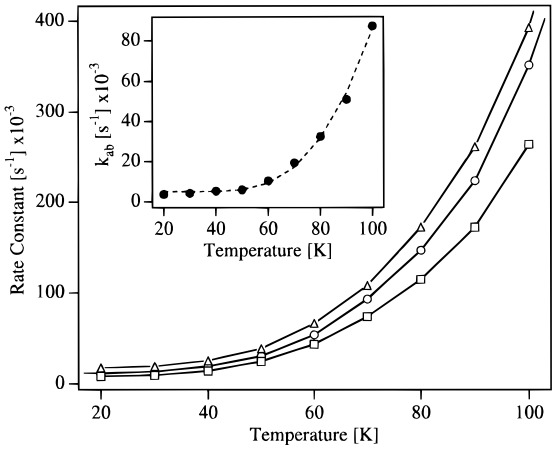

Figure 2. Rate constants for luminescence decay measured for doped crystals at 550 nm (circles) and 850 nm (triangles) and for pure ruthenocene at 550 nm (squares). The inset shows the difference in luminescence decay rate constants at 550 nm between the doped crystals and pure ruthenocene. The dashed line is the result of a fit of eq 1 to the points, as explained in the text.

The luminescence spectra in Figure 1 show important changes with temperature. The integrated luminescence intensity decreases with increasing temperature, as presented in the inset to Figure 1 for both doped crystals and pure ruthenocene samples. We observe a very similar decrease of integrated intensity with temperature for both types of samples. The most important change concerns the shape of the spectrum. As illustrated in Figure 1, the intensity of the low-energy band increases with temperature relative to the ruthenocene band. It is obvious that this band originates from a different luminophore, spectroscopically identified to be the nickelocene molecule (see below). The thermally activated energy transfer processes will be analyzed with a phenomenological model in the first part of the discussion.

Figure 2 shows luminescence decay rate constants as a function of temperature for nickelocene doped in ruthenocene and for pure ruthenocene crystals. The same doped crystal as in Figure 1 was used for the luminescence decay measurements at 550 and 850 nm. At the first wavelength, luminescence from the ruthenocene host dominates the spectrum, while at the second wavelength, we observe only the decay characteristics of nickelocene. For pure ruthenocene, the measurements were made at 550 nm and our results are in agreement with literature values.[5] We fitted only the part of the curves with intensities lower than 60% of the maximum intensity after the pulsed laser excitation in order to prevent artifacts and fast energy transfer processes from disturbing the single-exponential fits.[7] In the region of the curves used for the fits, the agreement between fit and experiment is excellent.

Figure 3a shows the low-temperature luminescence spectra of two doped crystals at 9 K, excited at 688.0 nm with a titanium−sapphire laser. The weak signal observed from the low-concentration doped crystal used for the measurements in Figures 1 and 2 is broad and symmetric with a maximum at 13 100 cm^{-1}, very similar to the near-IR band of the luminescence spectra in Figure 1. The same spectroscopic experiment for the higher concentration doped crystal (Ni/Ru 0.211) shows no band in the same wavelength range; this observation is also included in Figure 3a. We expect this result for the highly concentrated system, where no sensitized band was found under UV excitation. The comparison of the two traces obtained with 688.0 nm excitation confirms the presence of a weak band in the lightly doped crystal. At this wavelength only the nickelocene molecules will absorb, since the electronic origin for the

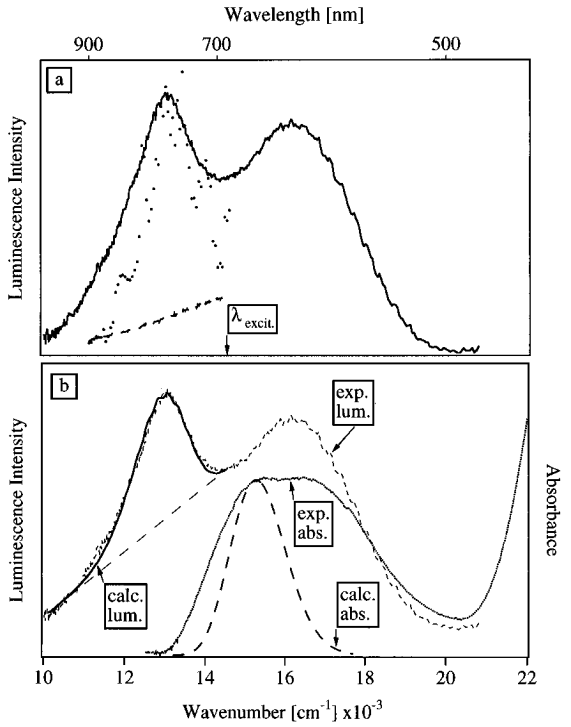

Figure 3. (a) Luminescence spectra of doped crystals under broad-band and selective excitation. The experimental luminescence spectrum at 80 K (broad-band UV excitation) is shown as a solid line. Dots indicate the selectively excited (λ_{excit} 688.0 nm) luminescence spectrum of a lightly doped (Ni/Ru 0.008) crystal at 9 K. The dashed line denotes the analogous spectrum for a heavily doped (Ni/Ru 0.211) sample. (b) Comparison of experimental and calculated spectra. The solid line indicates the calculated luminescence spectrum, compared to the experimental spectrum at 80 K (dashed line). The baseline used in the calculation is given by long dashes. The calculated absorption spectrum obtained with the same parameters is compared to the experimental spectrum measured at 9 K.

lowest energy transition of ruthenocene is at higher energy.[10] The selective excitation allows us to completely separate the luminescence spectrum of nickelocene from the overlapping spectrum of the ruthenocene host lattice. The intensity of the spectrum is lower by orders of magnitude than that for the sensitized luminescence observed in the same wavelength range in Figure 1, illustrating the efficient energy transfer from the host lattice which we use to amplify the weak signal from the dopant molecules. The band shape of the nickelocene luminescence spectrum will be analyzed in the second part of the discussion. The comparison of absorption and luminescence spectra in Figure 3b demonstrates that the infrared luminescence originates from nickelocene molecules: the spectra show a slight overlap at the electronic origin and the shape of the first absorption band is very similar to that of the low-temperature literature absorption spectrum of pure nickelocene.[11] The absorption spectrum contains less information on the lowest energy excited state because at least two electronic states are in the energy range of the first band, leading to a broad spectrum with two maxima.[8,9,11] The combination of absorption and luminescence spectra allows us to determine the energy of the first excited state of nickelocene as 14 300(300) cm^{-1}. The large Stokes shift of 2200 cm^{-1}, calculated from the luminescence maximum and the lower energy maximum of the absorption spectrum in Figure 3b, indicates significant structural changes in the emitting state.

(10) Riesen, H.; Krausz, E.; Luginbühl, W.; Biner, M.; Güdel, H. U.; Ludi, A. *J. Chem. Phys.* **1992**, *96*, 4131.
(11) Ammeter, J. H.; Swalen, J. D. *J. Chem. Phys.* **1972**, *57*, 678.

Discussion

(a) Energy Transfer from Ruthenocene to Nickelocene. The luminescence spectra in Figure 1 show that there is a thermally activated energy transfer from excited ruthenocene molecules to ground state nickelocene molecules, since the low-energy band increases in intensity relative to the high-energy band with increasing temperature. We rationalize these intensity changes and determine transfer rates from luminescence lifetime measurements with the phenomenological model presented in ref 12. In pure ruthenocene, excited molecules relax to the ground state by radiative or nonradiative intramolecular processes. In doped crystals, an additional relaxation pathway for ruthenocene involves the excitation of a nickelocene molecule by a nonradiative energy transfer process. The excited nickelocene centers then relax to the ground state either radiatively or nonradiatively. The rate constant for the total direct de-excitation of ruthenocene is k_a, that for nickelocene is k_b, and the rate constant for the nonradiative energy transfer is k_{ab}. The same model was applied to the luminescence decay characteristics of cobaltocene doped in crystals of ruthenocene.[7]

In order to determine the energy transfer rate k_{ab}, we calculated the difference between the luminescence decay rates at 550 nm for pure ruthenocene and for a doped crystal, the same approach as used for cobaltocene doped in ruthenocene,[7] and corresponding to eq 71 in ref 12. This wavelength is near the maximum of the ruthenocene luminescence band but far from the nickelocene band. The difference rates are identical to k_{ab} in the phenomenological model if we assume identical intramolecular relaxation rates for ruthenocene molecules in pure and doped crystals. This assumption is justified by the similar decreases in overall luminescence intensity with temperature observed for the two materials, shown in the inset to Figure 1, and by the identical luminescence decay rate constants at low temperatures, indicating similar quantum yields and absolute luminescence intensities. The values for k_{ab} are subject to considerable error, but they nevertheless show a consistent increase with temperature, as presented in the inset to Figure 2. The increase is largest at temperatures between 40 and 100 K, where we also observe the most important change in the relative intensities of the two luminescence bands in Figure 1. This observation supports our determination of phenomenological energy transfer rates from ruthenocene to nickelocene. The activation energy is obtained from a fit of eq 1 to the transfer rates $k_{ab}(T)$.

$$k_{ab}(T) = k_0 + A \exp(-\Delta E/kT) \qquad (1)$$

From the fit shown as a dashed line in the inset to Figure 2, we obtain an activation energy ΔE of 306(18) cm^{-1}. The constant k_0 represents an energy transfer rate without thermal activation. Its numerical value of $4.9(9) \times 10^3$ s^{-1} carries a large error, and we will not attempt to interpret it. The value of $6.6(1.8) \times 10^6$ s^{-1} found for A is poorly determined due to the lack of data at high temperatures, but it has little physical significance for energy transfer processes below 100 K.

The deactivation rate constant for nickelocene, k_b, could, in principle, be obtained from luminescence lifetime measurements of selectively excited nickelocene molecules. However, attempts to perform such measurements were unsuccessful due to the very weak luminescence of nickelocene when not sensitized by energy transfer from ruthenocene. The experimentally determined rate constants at 850 nm are higher than those determined at 550 nm and are included in Figure 2. The

(12) Powell, R. C.; Blasse, G. *Struct. Bonding* **1980**, *42*, 43. Section 3 (eqs 67−72) describes the phenomenological model for energy transfer.

significant overlap between the ruthenocene and nickelocene luminescence bands at this wavelength rules out a detailed analysis of the observed rates with our phenomenological model.

In summary, our analysis of the luminescence spectra and lifetimes confirms the presence of thermally activated energy transfer to nickelocene and allows the energy barrier to be estimated as 306(18) cm^{-1}, somewhat larger than the value of 140 cm^{-1} obtained for cobaltocene.[7] These similar activation energies indicate similar overall excitation transfer dynamics between ruthenocene and the first-row metallocenes. A microscopic analysis of the different activation energies and different energy transfer mechanisms is impossible because a number of different single-step and multistep energy transfer processes occur in doped crystals. They cannot be quantitatively analyzed from our spectroscopic data, but the phenomenological model used here leads to quantitative information on overall energy transfer rates in this organometallic solid.

(b) Emitting State of Nickelocene. The luminescence and absorption spectra of nickelocene in Figure 3 allow us to characterize the lowest energy excited state of nickelocene. Our analysis is based on unresolved spectra and will yield less information than the one for the emission spectrum of ruthenocene, a textbook example of a resolved spectrum.[5,6] Nevertheless, the comparison with the luminescence spectrum of cobaltocene doped in the same host lattice[7] will reveal important differences leading to different luminescence band shapes.

The luminescence and absorption spectra shown in Figure 3 determine the energy of the lowest excited state of nickelocene as 14 300(300) cm^{-1}. The large bandwidths of both the emission and absorption bands indicate significant differences between the ground and lowest energy excited states, implying different electron configurations for these two states. Ligand-field calculations predict $^1A_{1g}$ and $^3E_{1g}$ as potential emitting states.[8,9] The singlet excited state arises from a spin-flip within the same $(e_{2g})^4(a_{1g})^2(e_{1g})^2$ electron configuration as the ground state, a transition that would lead to much narrower luminescence and absorption bands than observed for our doped crystals down to the lowest temperatures. The molar absorptivity of the first absorption band in a series of organic solvents varies from 55 to 78 M^{-1} cm^{-1},[8,9] typical values for spin-allowed d−d transitions in centrosymmetric molecules. Therefore the lowest energy excited state is assigned as $^3E_{1g}$ ($(e_{2g})^4(a_{1g})^1(e_{1g})^3$ electron configuration) for nickelocene in the ruthenocene host lattice. The crystal spectra in Figures 1 and 3 do not show any transition equivalent to the weak ($\epsilon \approx 1$ M^{-1} cm^{-1}) feature observed on the onset of the $^3E_{1g}$ band in solution and assigned as $^1A_{1g}$.[9] In these solution spectra, the onset of the $^3E_{1g}$ band is at lower energy than the spin-flip transition to the singlet state, leading to the same lowest energy excited state as in our doped crystals. The $^3A_{1g}$ ground state is orbitally nondegenerate and therefore not susceptible to a Jahn−Teller effect, in contrast to the ground state of cobaltocene.[7] In the emitting state, three electrons are in the antibonding e_{1g} orbitals, leading to a significant weakening of the metal−cyclopentadienyl bonds.

The most important structural change in the emitting state is determined from a comparison of the experimental luminescence spectra and a model calculation. We use time-dependent theory as outlined in refs 13−15 to calculate both luminescence and absorption spectra. Only the totally symmetrical metal−cyclopentadienyl stretching coordinate is included in our model. The main progression in the luminescence spectrum of ruthenocene occurs along this vibrational mode,[6] and a correlation of metal−ring distance with increasing population of the antibonding e_{1g} orbitals was demonstrated for a series of 3d metallocenes.[16] These results underline the importance of the totally symmetric stretching vibration and support our assumption that the main structural change between the ground and emitting states, with different populations of the e_{1g} orbitals, is a nickel−cyclopentadienyl distance change. We describe the potential energy $V(Q)$ of the emitting state along the dimensionless nickel−cyclopentadienyl normal coordinate Q with eq 2.

$$V(Q) = {}^1/_2k(Q + \Delta Q)^2 + E_0 \qquad (2)$$

In this equation, k, ΔQ, and E_0 denote the wavenumber of the vibrational mode, the excited state structure change along Q, and the energy of the electronic origin transition, respectively. The wavenumber of the totally symmetrical vibration is 255 cm^{-1} for pure nickelocene, determined by Raman spectroscopy.[17] This value is used for both the ground and emitting state potential energy surfaces of nickelocene, making a correction for different zero-point vibrational energies in eq 2 unnecessary. A value of 14 350 cm^{-1} is used for the electronic origin E_0, determined from the spectra in Figure 3b. The excited state distortion ΔQ is the only adjustable parameter. The calculated luminescence spectrum in Figure 3b is in satisfactory agreement with both the selectively excited luminescence spectrum and the sensitized emission from nickelocene under broad-band UV excitation. A shift ΔQ of 3.61 along the dimensionless normal coordinate for the totally symmetric nickel−cyclopentadienyl vibrational mode is obtained from the calculated spectrum in Figure 3, corresponding to a Huang−Rhys parameter S of 6.5. The dimensionless shift ΔQ is converted to the normal coordinate in angstrom units[6] and leads to a difference in Ni−cyclopentadienyl distance δ_{Ni-cp} of 0.16 Å, a value similar to that for ruthenocene: 0.12 Å.[6] We use the same mass and definition of the normal coordinate as for ruthenocene.[6]

The numerical value for δ_{Ni-cp} defines an upper limit for this distance change because we do not take into account possible distortions along other normal coordinates with vibrational energies similar to that of the a_{1g} mode. Several of these modes contribute to the resolved vibronic structure observed for ruthenocene,[6] but the unresolved nickelocene luminescence spectrum makes such a detailed analysis impossible. In addition, we notice that the width at half-height of the luminescence band measured at 9 K with the 688.0 nm excitation is smaller by 500 cm^{-1} than the band obtained at 80 K with broad-band UV excitation, as shown in Figure 3a. This difference and the considerable overlap between emission and absorption spectra in Figure 3b indicate inhomogeneous broadening of the luminescence spectrum caused by nickelocene molecules at slightly different lattice sites. The inclusion of inhomogeneous broadening in the calculated luminescence spectrum would lead to a smaller distance change δ_{Ni-cp}, indicating again that our numerical value is an upper limit. The excitation wavelength of the titanium−sapphire laser used for the low-temperature luminescence spectrum in Figure 3 was specifically chosen to overcome inhomogeneous broadening as much as possible.

We used the parameters obtained from the luminescence spectrum to calculate the absorption band shape, included for comparison with the experiment in Figure 3b. The observed lowest-energy absorption band cannot be fully reproduced with

(13) Heller, E. J. *Acc. Chem. Res.* **1981**, *14*, 368.
(14) Lee, S.-Y.; Heller, E. J. *J. Chem. Phys.* **1979**, *71*, 4777.
(15) Zink, J. I.; Kim Shin, K.-S. *Adv. Photochem.* **1991**, *16*, 119.
(16) Haaland, A. *Acc. Chem. Res.* **1979**, *12*, 415.
(17) Chhor, K.; Lucazeau, G.; Sourisseau, C. *J. Raman Spectrosc.* **1981**, *11*, 183.

our model. It is much broader than the emission band and shows a double maximum, evidence for multiple electronic transitions leading to overlapping bands. Additionally, the orbitally degenerate $^3E_{1g}$ excited state is susceptible to a Jahn−Teller effect, which often has an important influence on the absorption band shape. Nevertheless, the onset of the absorption band up to the first maximum is reproduced by our calculation, indicating that the contribution of the lowest energy electronic level to the absorption band shape is correctly characterized by our model and confirming that the luminophore is in fact the nickelocene molecule.

The experimental Stokes shift can be used to obtain an independent estimate of the Huang−Rhys parameter S. Assuming identical harmonic potential energy surfaces with a vibrational frequency $\hbar\omega$ separated by an energy E_0, we obtain the Huang−Rhys parameter with eq 3. A value of 4.8 is obtained

$$S = \frac{(\text{Stokes shift}) + \hbar\omega}{2\hbar\omega} \tag{3}$$

for S with a vibrational energy of 255 cm^{-1} and the experimental value of the Stokes shift of 2200 cm^{-1}, in reasonable agreement with the value obtained from the calculated emission spectrum, especially in view of the experimental uncertainty of the Stokes shift and the simplifications leading to eq 3. This is a second experimental indication that the emission and absorption spectra in Figure 3b originate from the same molecular unit.

The comparison of the luminescence spectra of nickelocene and cobaltocene illustrates the fundamentally different electronic structures of these two metallocenes. Cobaltocene shows a distortion along a high-frequency e_{2g} vibration centered on the cyclopentadienyl ligand, leading to a very asymmetric band shape, whereas nickelocene shows a narrower, symmetrical spectrum, easily reproduced by a model involving only nickel−cyclopentadienyl distance changes between the ground and emitting states. The combination of luminescence spectroscopy and calculated band shapes provides a powerful approach to determine details of the electronic and geometrical structure of such related molecules, important information for the design of materials and rationalization of chemical reactivities.

Acknowledgment. This work was made possible by research grants from the NSERC (Canada) and FCAR (Province of Quebec). We thank Richard Leonelli (Département de physique, Université de Montréal) for the use of his titanium−sapphire laser system.

IC941346B